Chapter 17

Laser Ablation Applications in Ablation-Resistance Characterization of Materials

Yonggang Tong, Xiubing Liang, Shuxin Bai and Qing H. Qin

Additional information is available at the end of the chapter

http://dx.doi.org/10.5772/65108

Abstract

Owing to the rapid heating and large power intensity, the laser beams were successfully used to characterize the ablation-resistant performance of materials, which provided us more knowledge about the usability of materials in the ablation environment and developing protection against laser irradiation. In this chapter, we comparatively introduced some experimental methods for ablation-resistance characterization of materials. The fundamentals of laser-material interactions were discussed from the physical and chemical aspects to help understand the laser ablation mechanism. Finally, we presented some practical applications of laser ablation in ablation-resistance characterization of ultra-high-temperature ceramics (UHTCs) and ceramic matrix composites and discussed the laser ablation behavior and mechanism.

Keywords: Laser ablation, Ablation resistance, Laser-material interaction, Ceramic matrix composite, Ceramic coatings

1. Introduction

A light amplification by stimulated emission of radiation (laser) is a device that emits light through the process of stimulated emission. Owing to the advantages of laser radiation over conventional mechanical and thermal techniques, it was suggested to be used as a manufacturing tool after the development of the first laser. Over the last few decades, great effects have been made to develop various laser devices. According to the lasing medium, the lasers can be classified as gas lasers, liquid lasers, solid-state lasers, semiconductor lasers, and free-electron lasers.

Because of the unique energy sources characterized by spectral purity, spatial and temporal coherence, and high intensity, the laser beams have captured significant attention and widely been used in matrix-assisted laser desorption/ionization, laser surgery, micro-fabrication, pulsed laser deposition, etc. [1]. Recently, they were successfully used to evaluate the ablation-resistant performance of materials, which provided us more knowledge about the usability of materials in the ablation environment and developing protection against laser irradiation. A great amount of work on laser ablation of polymer-based composites, ultra-high-temperature ceramics (UHTCs), ceramic-based composites, and ablation-resistant coatings has been reported. The linear and mass ablation rates of these materials were tested using the laser ablation method, and the laser ablation behavior and mechanism were investigated by experiments and numerical simulation.

In this chapter, we firstly made a simple introduction of the ablation-resistance characterization methods for materials and compared the advantages and disadvantages of these methods with laser ablation method. To help understand the laser ablation mechanism of ultra-high-temperature materials, the fundamentals of laser-material interactions were discussed from the physical aspects and chemical aspects. The physical aspects mainly involved the absorption of laser radiation, heating and propagation, melting, vaporization, and solidification. The chemical aspects mainly involved the decomposition of the phases in materials and the reaction of the materials with the atmosphere. Finally, we presented some practical applications of laser ablation in ablation-resistance characterization of materials based on our research and some relevant literatures. The ablation rates of materials under different laser parameters were tested. The morphologies of the ablated surface were observed by electron microscopes, and the ablation mechanism was discussed.

2. Ablation-resistance characterization methods for materials

Advanced aerospace structures and anti-ablation components, such as nose caps, sharp leading edges, and rocket engines for hypersonic aerospace vehicles, suffer from high heat fluxes and pressure, severe thermal shock, and perhaps high-speed erosion of ceramic particles in their working conditions [2]. The serving temperatures of these components may increase rapidly from the room temperature to over 2000 °C and last from several seconds to several hundreds of seconds. Materials with outstanding mechanical and ablation-resistant properties are required for these structures and components. Refractory metals, carbon-based composites (graphite and C/C composite), ultra-high-temperature ceramics, and composites are potential candidates due to their extremely high melting points, high-temperature mechanical strength, and outstanding ablation resistance. Due to the special serving environments, it is necessary to validate the ablation properties of these materials. Ablation resistance has been one of the most important properties in evaluating the usability of these materials. Great efforts should be devoted to the investigation on the ablation-resistance characterization, microstructure evolution, and ablation mechanism of these materials before their practical applications in the ablation environments.

http://dx.doi.org/10.5772/65108

Normally, ablation resistance of materials can be investigated by ballistic flight experiments and ground-based simulation experiments [3]. Ballistic flight experiments can evaluate the ablation properties of materials in a real serving condition. However, this experiment is seldom used to characterize the ablation resistance of materials because of the considerable cost. By contrast, ground-based simulation experiments are more practical to investigate the ablation resistance of materials. The main ground-based simulation experimental methods are wind tunnel ablation testing, plasma arc-jet ablation testing, and oxyacetylene flame ablation testing [4–6]. Wind tunnel ablation testing can simulate the ablation conditions of high enthalpy and strong gas flows, but it cannot simulate the fully representative flight envelope in terms of Mach and Reynolds number [4]. Plasma arc-jet ablation testing [5] can partially simulate the reentry environment. Nevertheless, the parameters are simple. Additionally, both wind tunnel and plasma arc-jet ablation testing are costly. By contrast, oxyacetylene torch testing is a simple and low-cost method [6, 7]. It is widely used in labs to provide a primary evaluation about the ablation properties of materials. However, the ablation temperature of oxyacetylene torch test is limited by the flame temperature (about 3000°C), and the combustion products of the oxyacetylene flame include O_2, CO_2, O, OH and H_2O [7], which may affect the ablation resistance of materials.

Recently, the laser beams were successfully used to evaluate the ablation-resistant performance of materials. A great amount of work on laser ablation of polymer-based composites, ultra-high-temperature ceramics, ceramic-based composites, and ablation-resistant coating has been reported. The published literatures demonstrate that laser ablation is a simple and cost-effective method to characterize the ablation resistance of materials. Irradiated by the laser beams, materials can be rapidly heated to a very high temperature. Additionally, the laser ablation testing does not introduce any combustion products and mainly provides a rapid thermal impact, which is beneficial to analyze the ablation behavior and mechanism of the materials.

3. Fundamentals of laser-material interactions

Laser-material interactions are very important to understand laser ablation process of materials. Irradiated by the laser beams, the substrate materials absorb the irradiation energy. Absorption of radiation in the materials results in various effects such as heating, melting, vaporization, and plasma formation. The extent of these effects primarily depends on the characteristic of electromagnetic radiation and the thermophysical properties of the substrate materials [8]. The laser parameters include intensity, wavelength, angle of incidence, spatial and temporal coherence, illumination time, and polarization, whereas parameters of the substrate materials include absorption of the laser energy, thermal conductivity, specific heat, and density. They all should be taken into account in order to understand in details the effects of laser ablation processing on the substrate materials tested. In addition to these physical aspect effects, the substrate materials are believed to react with the atmosphere under the thermal impact. The phases in the substrate materials will be changed, and they even decompose and vaporize, which greatly affects the ablation resistance of the substrate material. Thus,

the laser-material interactions are very complex, and only in some simple cases, the laser can be merely seen as a heat source. The laser-material interactions should be comprehensively considered from the physical aspects and chemical aspects.

3.1. Physical aspects

3.1.1. Absorption of laser radiation

When laser beam strikes the surface of the substrate material, a portion of laser energy will be reflected from the interface due to the discontinuity in the real index of refraction, and the rest will be transmitted into the material. The reflectivity of a given material depends on the frequency of the light source through the dispersion relation of its index of refraction. **Figure 1** [9] presents the variation of reflectivity with the wavelength of some common metallic materials. As indicated in **Figure 1**, the reflectivity of the material generally increases with increasing wavelength. Thus, the laser energy is strongly absorbed by materials at shorter wavelengths.

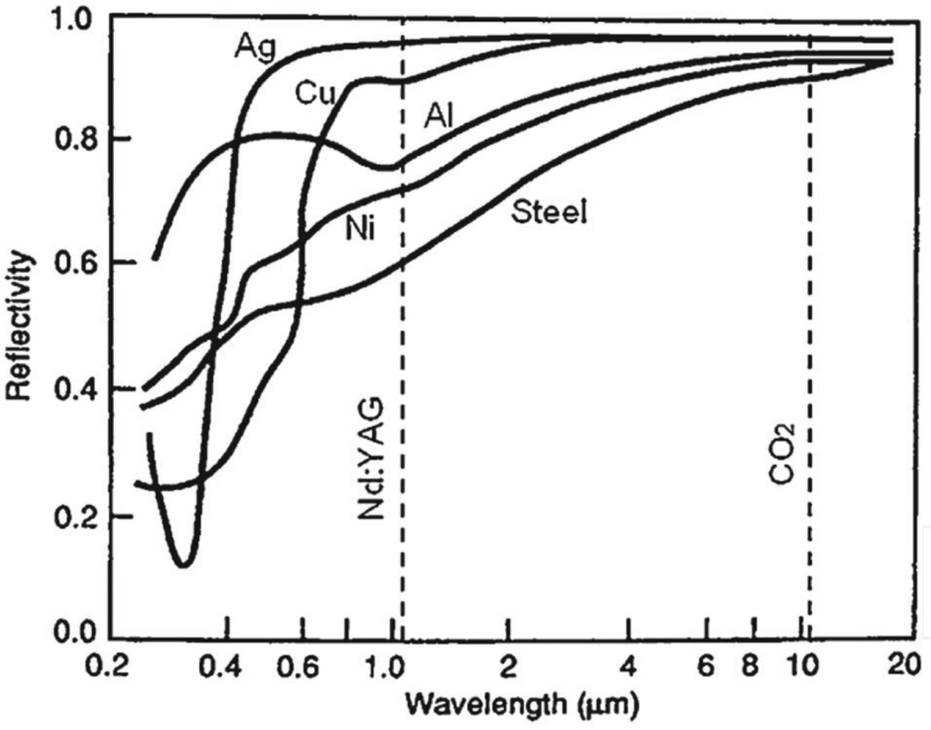

Figure 1. Variation of reflectivity with wavelength for some metallic materials.

In addition to the reflected fraction, the laser irradiation on the surface of substrate material leads to the excitation of free electrons (in metals), vibrations (in insulators), or both (in semiconductors) [8]. The excitation results in an energy increase in the system, and this excitation energy is rapidly converted into heat for a very short time period. That is the fraction of laser irradiation absorbed by the substrate materials.

http://dx.doi.org/10.5772/65108

Once inside the materials, absorption causes the laser intensity to decay with depth at a rate determined by absorption coefficient of the substrate materials α. In general, α is a function of laser's wavelength and temperature. However, for constant α, the laser intensity, I, decays exponentially with depth z according to the Beer-Lambert law [10]:

$$I(z) = I_0 e^{-\alpha z} \tag{1}$$

where I_0 is the intensity just inside the surface after considering reflection loss. Considering the depth at which the intensity of the transmitted light drops to $1/e$ of its initial value at the interface, the optical penetration or absorption depth can be conveniently defined as $\delta = 1/\alpha$. **Figure 2** [11] shows the optical absorption depth as a function of wavelength for some common materials, such as metals and semiconductors. The important thing to note from **Figure 2** is that the absorption depths are quite small relative to bulk material dimensions. Thus, absorption of the laser energy only happens at the surface of materials.

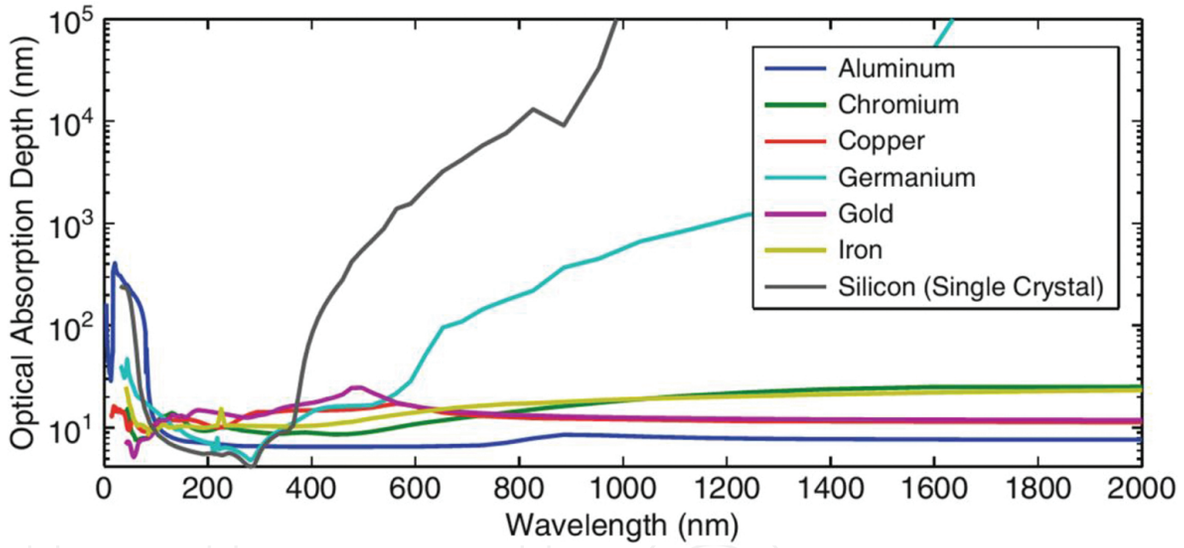

Figure 2. Optical absorption depths of some materials for different wavelengths.

3.1.2. Heating

Once the laser energy is absorbed by the substrate materials, it is followed by various heat transfer processes such as conduction into the materials, convection, and radiation from the surface. The most significant heat transfer process is the heat conduction into the material. The heat conduction from the surface to the inner of materials establishes a temperature distribution in the material depending on the thermophysical properties of the material and laser parameters. Ignoring the convective and radiative energy transport, the temperature distribution T in a material can be given by the heat conduction equation, which, in 2D, can be written as [12],

$$\rho(T)C_p(T)\frac{\partial T(x,y,t)}{\partial t} = \nabla\left[k(T)\nabla T(x,y,t)\right] + Q(y,t) \tag{2}$$

where x and y are the space coordinates and k, C_p and ρ are the thermal conductivity, specific heat at constant pressure, and mass density of the target material, respectively. Here, the source term $Q(y,t)$ is the laser radiation absorbed by the substrate material and is expressed as [13],

$$Q(y,t) = I_s(1-R)\alpha\exp(-\alpha y) \tag{3}$$

where α and R are the absorption and reflectivity coefficient of the substrate material, respectively, y is the spatial coordinate in the direction normal to the sample surface, and I_s is the laser irradiance at the sample surface. According to Bulgakova and Bulgakov [14], I_s is expressed as,

$$I_s(t) = I(t)\exp\left[-\omega(t)\right] \tag{4}$$

Based on the above equations and thermophysical properties of the materials, the temperature distribution caused by the laser energy absorption at the material surface and subsequent conduction into the body material can be calculated. Finite element analysis and some numerical calculation methods can be used to solve these equations. For composite materials, the temperature distribution plays a more important role to analyze the ablation behavior and mechanism. The phases in the composites have different thermophysical properties, which cause a quite different temperature distribution in different phases, and consequently, the phases may present different ablation behavior and mechanism.

3.1.3. Melting

Irradiated by laser beams with relatively large laser power densities, surface temperatures of the materials may reach their melting temperatures (without surface evaporation). The melting of materials significantly depends on their melting points. **Figure 3** shows the melting points of some high-temperature materials [15]. The surface of pure metals melts once the surface temperature reaches their melting temperatures. Nevertheless, the surface melting of composite materials is greatly influenced by the phase composition of the materials. The phases in the composites have different melting points, which can get melting in turn with increasing laser power densities or impulse time. The former melted phases may react with some other phases or the atmosphere. New substances may be produced and affect the surface melting and phase composition of the materials.

http://dx.doi.org/10.5772/65108

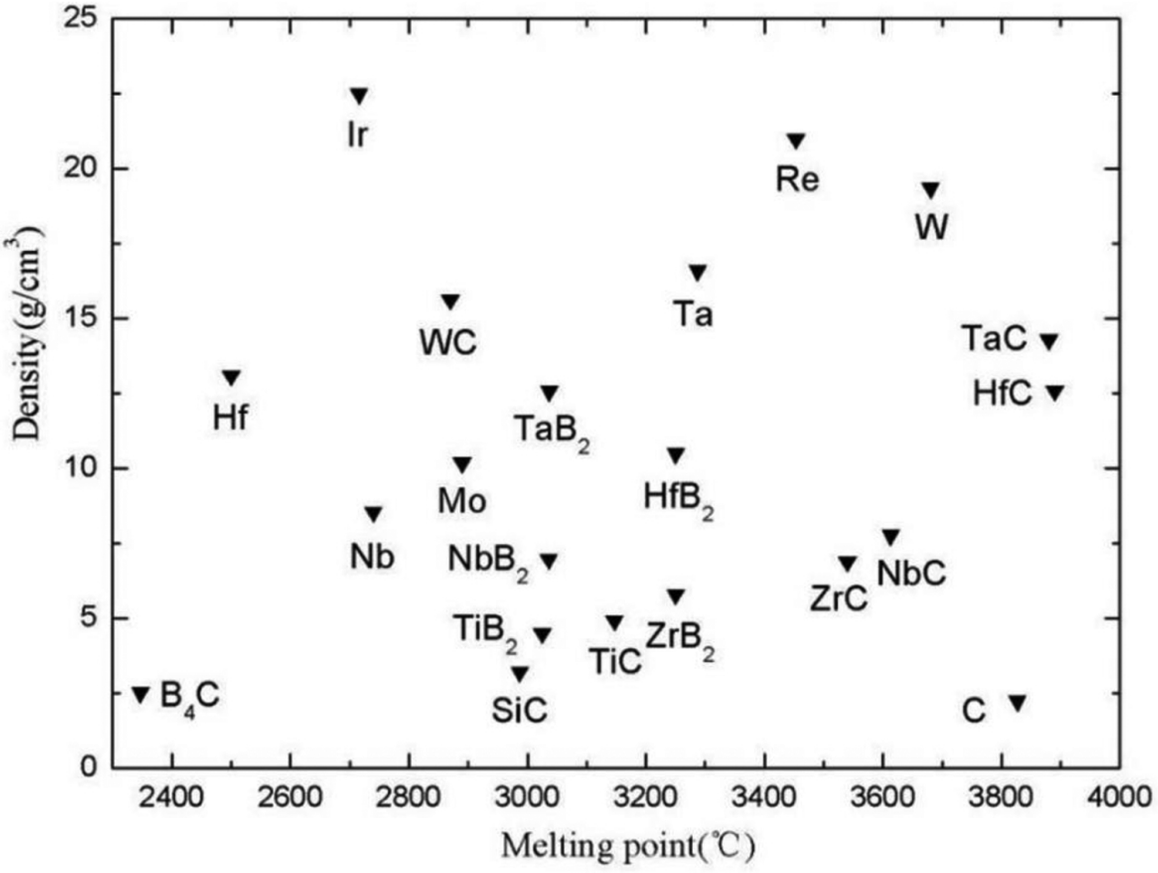

Figure 3. Melting points of some high-temperature materials.

3.1.4. Vaporization

If the incident laser intensity is sufficiently high, the surface of materials can be heated to its boiling temperature, and material removal by evaporation is caused by the laser ablation. The melting depth reaches the maximum value once the surface temperature reaches the boiling point. Further increase of laser power density or pulse time causes the more severe evaporative material removal from the surface without any further increase in the melting depth. The maximum melting depth (z_{max}) at which the surface reaches the boiling point can be calculated as follows [16]:

$$ierfc\left(\frac{Hz_{\max}}{kT_b\sqrt{\pi}}\right)=\frac{T_m}{T_b\sqrt{\pi}} \tag{5}$$

where Hz_{max} is the maximum melting depth, T_b and T_m are the boiling and melting temperatures of the substrate materials, and k is the Boltzmann constant.

Once the vaporization is initiated at the surface of the material, the continued laser irradiation causes the liquid-vapor interface to move inside the material with the evaporative removal of

material from the surface above the liquid-vapor interface. Assuming the thermal ablation as vaporization, the flow of material vaporized from the surface of a body at temperature T can be calculated according to the Hertz-Knudsen equation [13], leading to an ablation rate ϑ as [17],

$$\vartheta(T) = (1-\beta)\sqrt{\frac{m}{2\pi m k_B T}}\frac{p_0}{\rho}\left[\frac{L_V}{k_B}\left(\frac{1}{T_b}-\frac{1}{T}\right)\right] \tag{6}$$

where T_b is the boiling temperature at pressure p_0, k_B is the Boltzmann constant, β is the back flux coefficient, and L_V is the latent heat of vaporization of the material.

3.1.5. Plasma formation

Irradiated by the laser beams with sufficiently large intensity, a great amount of surface evaporation occurs as mentioned in the previous sections. Once the vaporization takes place, the interactions between the as-produced vapor and the incident laser beam become important in determining the overall effect of the laser irradiation on the substrate material. Interaction of the laser with the vapor can lead to the ionizing of the vapor. The highly ionized vapor is termed as plasma. In dynamic equilibrium, the degree of ionization ε in the vapor can be expressed by the Saha equation [18]:

$$\frac{\varepsilon^2}{1-\varepsilon} = \frac{2g_i}{g_a N_g}\left(\frac{2\pi m k_B T}{h^2}\right)^{\frac{3}{2}}\exp\left(-\frac{E_i}{k_B T}\right) \tag{7}$$

with $\varepsilon = N_e/N_g$ and $N_g = N_e + N_a$. Here, N_e and N_a are the number densities of electrons and atoms/molecules, respectively; g_i and g_a are the degeneracy of states for ions and atoms/molecules; and E_i is the ionization energy.

The vapor and the plasma can absorb and scatter the laser radiation, which changes the actual flux received by the substrate surface. Recoil from the vapor and plasma can also generate shock waves in the substrate material, which may cause plastic deformation and work hardening [19]. Expulsion of any remaining molten material as well as initiate shock waves can be further caused by the recoil as well. In this chapter, laser ablation method is used to characterize the ablation-resistance performance of materials. It is not reasonable to choose too large laser intensity. Therefore, we make very little consideration of plasma formation.

3.1.6. Recondensation and resolidification

Irradiated by the laser beams with large power densities, the material surface is heated to a rather high temperature, and significant surface evaporation and sometimes plasma take place, which makes a positive pressure over the ablated surface. Surface temperature increment from 300 to 3500 K can lead to an enormous vapor pressure increase from 10 bar to almost 160 bar

http://dx.doi.org/10.5772/65108

for a time interval comparable with the pulse duration (pulse D 55 ns). The vapor and plasma may eject from the ablated center under the driving of the positive pressure and subsequently recondensate on the surface of the material. Besides, laser ablation is usually carried out in the air atmosphere or some reactive atmospheres. Some new phases may be formed due to the chemical reaction between the vapor and the ambient gas. The new reaction-formed chemical compounds may also condensate on the surface of the materials.

As we mentioned above, recoil of the vapor and plasma can cause further expulsion of the remaining molten material. The molten materials expulsed from the ablated center and remaining in the ablated center resolidify and also form some new phases on the surface of materials.

Resolidification of the molten materials and condensation of the vapor and plasma are very important to analyze the morphologies of the ablated surface of the materials. They may form some thin films and nanoparticles and alter the topography at the rim and surrounding areas of the ablated region.

3.2. Chemical aspects

In addition to the physical aspects, the substrate materials and ablation products are believed to react with the ambient gas, and some new compounds may be formed during the laser ablation process. Thus, the laser ablation should also be discussed from the chemical aspects.

Normally, laser ablation is carried out in the air atmosphere. Irradiated by the laser beams, the substrate material is heated to a high temperature, and the phases in the materials can react with the oxygen in the air atmosphere. For carbon-based materials, such as graphite and C/C composite, the reaction of the materials with oxygen produces gas products, CO and CO_2, which are liable to eject from the ablated surface. The substrate materials are severely ablated with a large decrease of external dimensions. However, for the refractory alloys and refractory-based ceramics, refractory oxides are produced due to the oxidation reaction. The refractory oxides have high melting points and low evaporation rates at high temperatures (see in **Table 1** [20]). Especially, the oxygen permeabilities in these oxides are very small. The substrate materials can be isolated from most of the oxygen, and thus, the substrate material can be prevented from the reaction of oxygen in the air atmosphere. Taking this into consideration, the former reaction-formed oxides provide protection for the substrate materials and reduce the damage of the laser ablation.

Oxides	Melting point (°C)	Density (g/cm^3)	Thermal expansion (ppm/°C)	Evaporation rate (10^{-6} m/h) 10^{-5} at 1650 °C	Oxygen permeability (g/cm s) 10^{-10} at 1800 °C
HfO_2	2810	9.68	6.8	6.7	46
ZrO_2	2700	5.6	7.5	670	30
Y_2O_3	2460	5.03	6.8	–	2.0
Al_2O_3	2015	3.98	8.1	–	–
SiO_2	1728	2.32	0.5	–	–

Table 1. Properties of some refractory oxides.

Irradiated by laser beams with very large intensity, the substrate materials may be heated to very high temperatures over the decomposed temperature of some phases. Taking carbon and SiC, for example, they sublimate once heated over 3827 and 2987 K, respectively [21]. The gas products eject from the ablation surface and may also result in a severe damage to the substrate materials. Besides, these gas products may also recondensate and form some thin films and nanoparticles at the rim and surrounding areas of the ablated region. Understanding these chemical reactions during laser ablation plays a great role to analyze the final morphologies of the ablated surface and study the ablation mechanism of the substrate materials. It should be noted that the above reactions are greatly affected by the temperatures during laser ablation, which depends on the laser parameters (pulse duration, energy, and wavelength), the substrate materials' properties, and the surrounding environment condition.

4. Laser ablation applications in ablation-resistance characterization of materials

4.1. Carbon fiber-reinforced ceramic matrix composites

Carbon fiber-reinforced ceramic matrix composites, combined with the excellent properties of carbon fiber and high-temperature ceramics, are one of the most promising candidate materials for high-temperature components due to their unique properties such as relative low density, low coefficient of thermal expansion, high specific strength/modulus, and excellent ablation resistance. In this section, we chose C/SiC composite as an example and comprehensively discussed the laser ablation behavior and mechanism. In addition, some recent work on laser ablation of C/C-ZrC composite in o*u*r group and by some other researchers was reviewed.

4.1.1. Production of C/SiC composite and the laser ablation test

C/SiC composite for laser ablation testing was fabricated using a polymer infiltration and pyrolysis (PIP) method [22] by the Key Laboratory of Advanced Ceramic Fibers and Composites (National University of Defense Technology, Changsha, China). Three-dimensional braided carbon fiber preform was used as the reinforcement. Polycarbosilane (PCS) was chosen as the precursor of SiC matrix. Divinylbenzene (DVB) was used as solvent and cross-linking reagent for PCS. The preparation process of the composite contained three steps: (1) the carbon fiber preforms were immersed into the PCS/DVB solution and infiltrated with the PCS/DVB solution in vacuum at room temperature; (2) the preforms filled with PCS/DVB solution were cured at 150 °C; and (3) the cured preforms were pyrolyzed at 1200 °C to form the SiC matrix in an inert atmosphere. In order to densify the composites, the other several infiltration-cure-pyrolysis cycles were repeated. The as-produced C/SiC composite is composed of carbon and SiC (determined by XRD) and generally dense with two kinds of pores. One is small distributing in the intra-fiber bundles, and the other is larger locating in the interfiber bundles (**Figure 4**).

http://dx.doi.org/10.5772/65108

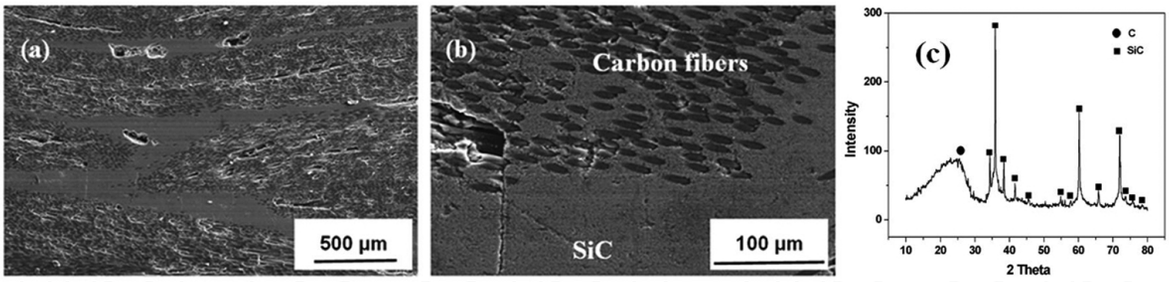

Figure 4. Cross-sectional microstructure (a and b) and XRD diffraction patterns (c) of C/SiC composite.

Ablation properties of the as-produced C/SiC composite were tested using a pulsed laser in the air. The laser ablation equipment is an Nd:YAG pulsed laser (wavelength 1.064 μm) with the following parameters: frequency 20 Hz and pulse width 1 ms. During the ablation testing, the C/SiC composite was located in a test chamber and was then vertically irradiated by the pulsed laser. The ablation depth of C/SiC composite was given by the thickness changes before and after the ablation test, which was measured by a microscope.

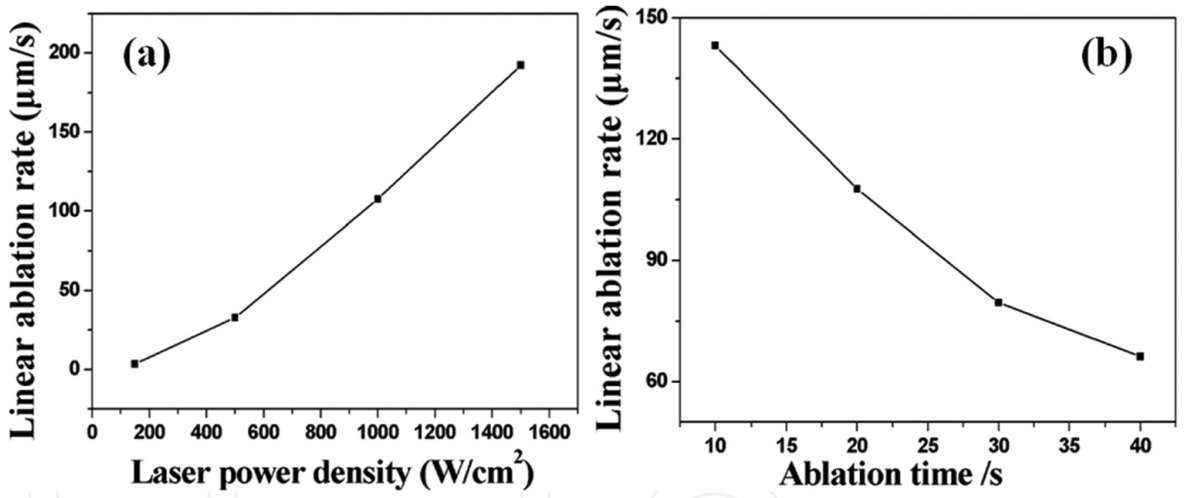

Figure 5. Linear ablation rates of C/SiC composite versus (a) laser power densities and (b) time.

4.1.2. Laser ablation resistance of C/SiC composite

Linear ablation rates of C/SiC composite tested with different laser power densities are shown in **Figure 5(a)**. It is indicated that the linear ablation rates of the composites increase with increasing laser power densities. During the ablation process, the laser energy is absorbed by the composite. Along the heat penetration depth and conduction width, the conduction laser energy decreases progressively from their input value, which in turn affects the corresponding temperature distribution. The larger the testing laser power density is, the higher the temperature of the composite is heated to be and the greater the heat penetration depth is. Therefore, the linear ablation rates increase with increasing of the laser power densities.

Ablation resistance of C/SiC composite was also tested for different time periods. **Figure 5(b)** shows the linear ablation rates of C/SiC composites tested for different time periods with laser power density of 1000 W/cm^2. It is indicated that the linear ablation rates of C/SiC composites decrease with an increase of ablation time.

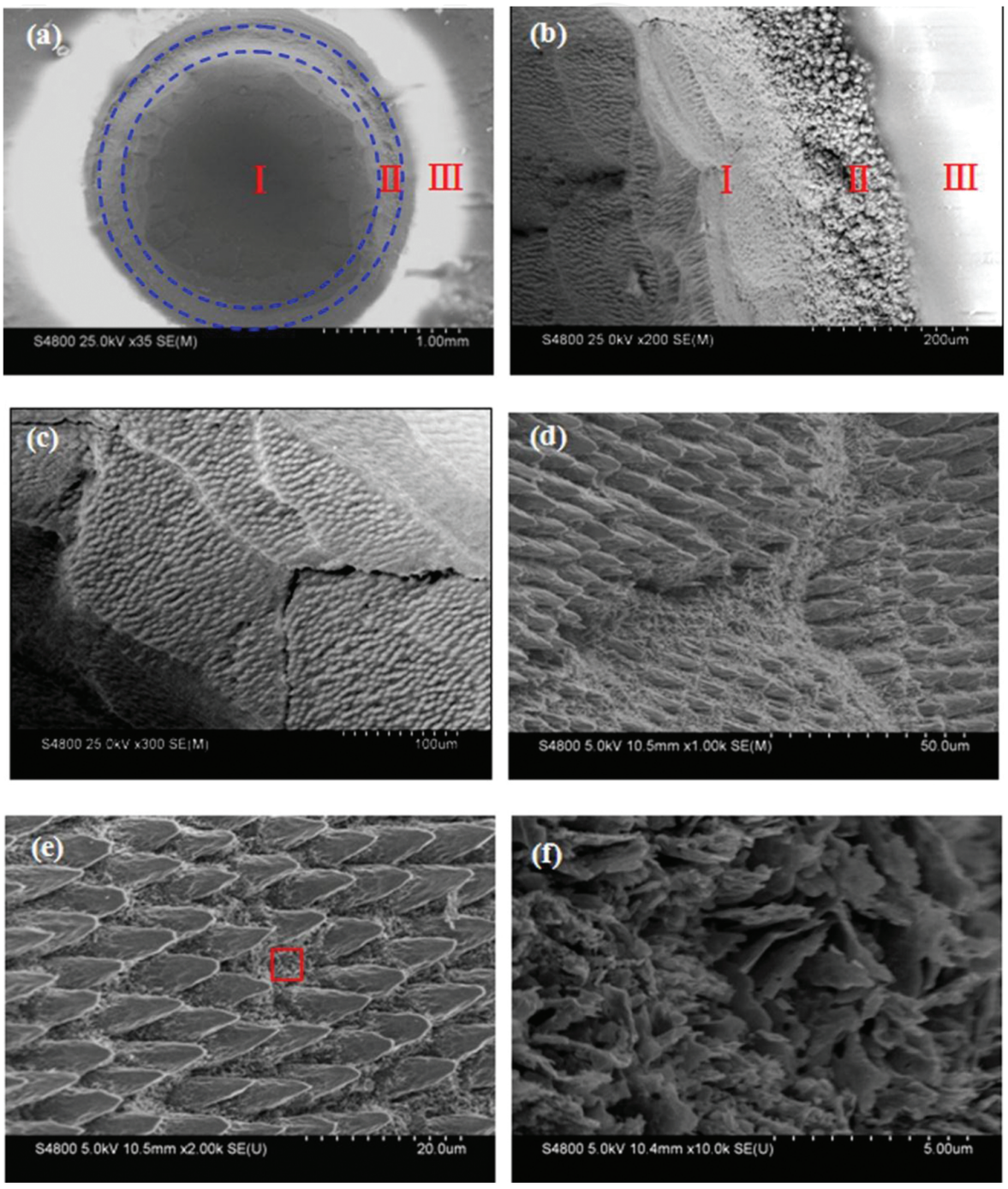

Figure 6. Ablated surface morphologies of C/SiC composite at 1000 W/cm^2 for 20 s (a and b) three ablated regions on the ablated surface, (c) macro-morphologies of the ablation center, (d and e) large magnification morphologies of ablation center, and (f) large magnification of the marked area in (e).

http://dx.doi.org/10.5772/65108

4.1.3. Microstructure morphologies of the ablated composite [23]

Figure 6 shows the surface morphologies of the C/SiC composite after laser ablation testing at 1000 W/cm^2 for 20 s. Three ablated regions can be identified on the ablated surface of the composite according to the difference of the morphologies: region I ablation center with a deep pit, region II transitional zone with a lot of spheric particles, and region III ablation edge covered by a white glassy layer (**Figure 6(a** and **b**)). Detailed scanning electron microscope (SEM) characterization of region I (**Figure 6(c** and **d)**) shows that the ablation center region exhibits a needle-like structure with taper-ended carbon fibers standing on the ablated surface filled with some nanostructure sheet. In order to determine the composition of the above three ablated regions and the nanostructure sheet, EDS analysis was carried out. The results indicate that the nanostructure sheet is nanocarbon sheet composed of pure carbon. The spheric particles in the transitional region are composed of silicon and carbon owning the atom proportion of 54.47:45.53, which are SiC particles. The white layer covered on the ablated surface of region III ablation edge is SiO_2 composed of silicon and oxygen.

During the laser ablation testing, the center region of the composite was instantly heated to a very high temperature, which was thought to be approximately higher than 3500 °C due to the large amount of ablated carbon fibers observed in the ablated center region. At such a high temperature, SiC matrix in the composite decomposes and sublimates, which forms a hot mixture of gases and vapors. Carbon fibers in the composite also get to its sublimation temperature to form a carbon vapor. The decomposition and sublimation of SiC and carbon fibers can be described as the following reactions:

$$\mathrm{SiC(s)} \rightarrow \mathrm{Si(g)} + \mathrm{C(g)} \tag{8}$$

$$\mathrm{SiC(s)} \rightarrow \mathrm{SiC(g)} \tag{9}$$

$$\mathrm{C(s)} \rightarrow \mathrm{C(g)} \tag{10}$$

Because the ablation testing was performed in the air, carbon fibers and SiC matrix are believed to react with the oxygen in the atmosphere and form the products of CO, CO_2, SiO, and SiO_2 due to the reaction with oxygen. The possible reactions that take place in the oxidation of carbon fibers and SiC matrix are as follows:

$$\mathrm{SiC(s)} + \mathrm{O_2(g)} \rightarrow \mathrm{SiO_2(g)} + \mathrm{CO(g)} \tag{11}$$

$$\mathrm{SiC(s)} + \mathrm{O_2(g)} \rightarrow \mathrm{SiO(g)} + \mathrm{CO(g)} \tag{12}$$

$$C(s) + O_2(g) \rightarrow CO_2(g) \tag{13}$$

$$C(s) + O_2(g) \rightarrow CO(g) \tag{14}$$

Among the products of the above reactions, SiO, CO, and CO_2 are gases. SiO_2 immediately gasifies due to its low boiling temperature, 2230 °C [24]. These gas products result in a positive pressure atmosphere on the ablation surface. Oxygen in the atmosphere on the ablation surface can be instantly exhausted, and the oxygen in the outside atmosphere hardly diffuses into the atmosphere on the ablation surface because of the positive pressure kept by the gasses and vapors produced according to Eqs. 8–14. Therefore, the oxidation of SiC and carbon fibers just takes place at the very beginning and is made no consideration in the subsequent analysis.

Ablation of the composite is greatly influenced by the temperatures functioning on the ablated areas. Irradiated by the laser, the center area of C/SiC composite was heated to the highest temperature, and it was severely ablated. Because the carbon fibers are thermally more stable than the SiC matrix, carbon fibers with taper ends protruded on the ablation surface without the SiC matrix as shown in **Figure 6(c)**. Inside the composite under the ablated center region, the heat absorbed from the laser penetrates into the inner of the body composite along the direction of the laser beam. It is known from Section 3 that the penetrated heat decreases with the increasing of the penetration distance. Thus, the temperature at this region decreases with the increase of the heat penetration depth. The ablation of carbon fibers is gradually alleviated due to the temperature decrease and finally avoided along the heat penetration direction. Therefore, carbon fibers on the ablated surface in the center region present a needled-like structure with taper ends. Though the ablation of carbon fibers is alleviative and avoidable along the heat penetration direction, the temperature at this region is high enough to lead to the SiC decomposition. Therefore, lots of grooves without SiC matrix are formed among the carbon fibers which are lower than the carbon fibers' taper ends. With further increase of the depth, the temperature in the grooves decreases. At a certain depth, the temperature reaches a critical value, and the decomposition of SiC matrix stops. The SiC decomposition according to Eq. 8 and carbon fiber sublimation according to Eq. 10 produce a carbon-rich atmosphere on the ablation surface. In the grooves among carbon fibers, the SiC matrix can decompose while the temperature is not high enough to sublimate the carbon fibers. Some nanocarbon sheet is deposited at the bottom region of the grooves (**Figure 6(c** and **d)**), which is quite similar to the preparation of carbon nanotubes by laser ablation method [25].

Different from the ablated center region, the conducted heat and the corresponding heat penetration depth at region II transitional zone of the ablation surface are much smaller. It is not high enough to lead to the decomposition, vaporization, and sublimation of SiC matrix. The mixed gases of C, Si, and SiC escaped from the ablation center region can be cooled down in this area with relatively lower temperature. SiC grains re-nucleate and grow to spherical particles (see **Figure 6(b)**). Though the temperature at the transitional zone is lower than the ablation center and cannot lead to the decomposition, vaporization, and sublimation of SiC

matrix, it is still believed to be high enough to volatilize the SiO_2 phase. Thus, no SiO_2 was found at the transitional zone.

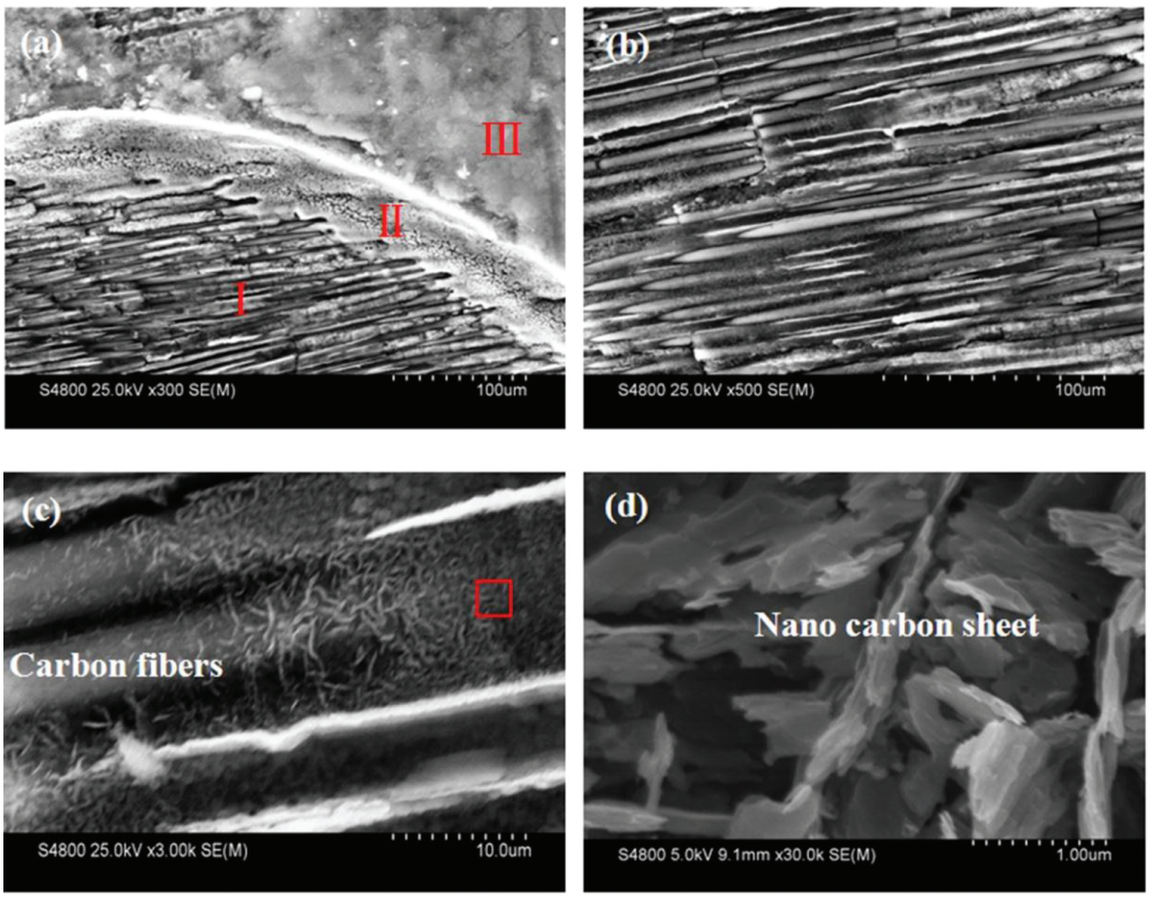

Figure 7. Surface morphologies of C/SiC composite ablated at 150 W/cm^2 for 20 s.

Compared with the ablated center region and the transitional zone, the heat at region III ablation edge is only conducted form the ablation center, and the temperature is the lowest. The oxygen in the outside atmosphere can continuously diffuse into the atmosphere over the composite surface of this area, and the C/SiC composite is oxidized. Due to the lowest temperature, SiO_2 produced from the oxidation of SiC matrix cannot be volatilized. The composite at this region is covered by a white glassy SiO_2 layer (**Figure 6(a)**). The electrical conductivity of SiO_2 is not very well. Thus, the layer shows a white fuzzy pattern under the scanning electron microscope.

Figure 7 shows the surface morphologies of the C/SiC composite ablated at 150 W/cm^2 for 20 s. As can be seen, most carbon fibers remain their original shape without obvious ablation damage, which is owing to the low temperature heated by laser beam with low laser power density. Nevertheless, some nanocarbon sheets were found on the ablated surface and the SiC matrix among the carbon fibers decomposed (the same situation on the surface of the composite ablated at 1000 W/cm^2), which indicates that the temperature on the composite surface ablated at 150 W/cm^2 is high enough to induce the decomposition of SiC matrix. However, that

temperature is not sufficient to lead to the sublimation of the carbon fibers, and they still remain the original shapes. The ablated surface mainly shows the ablation of SiC matrix.

4.1.4. Laser ablation mechanism

Laser ablation of composite materials is very complicated and influenced with the laser power density and properties of phases in the composite substrate. In order to further understand the laser ablation processes of the C/SiC composite, an ablation model based on the previous characterization results and discussion was proposed (**Figure 8**).

As aforementioned, the temperature at the ablated center during laser ablation is the highest. The composite is heated to a very high temperature over 3500 °C. The SiC matrix reaches its decomposition and sublimation temperatures to form a hot mixture of gasses and vapors, and the carbon fibers get to its sublimation temperature to form a carbon vapor, which results in a positive carbon-rich atmosphere on the ablated surface. The carbon fibers are thermally more stable than the SiC matrix and carbon fibers with taper ends protrude on the ablation surface without the SiC matrix. Nanocarbon sheet is formed in the grooves among the protuberant

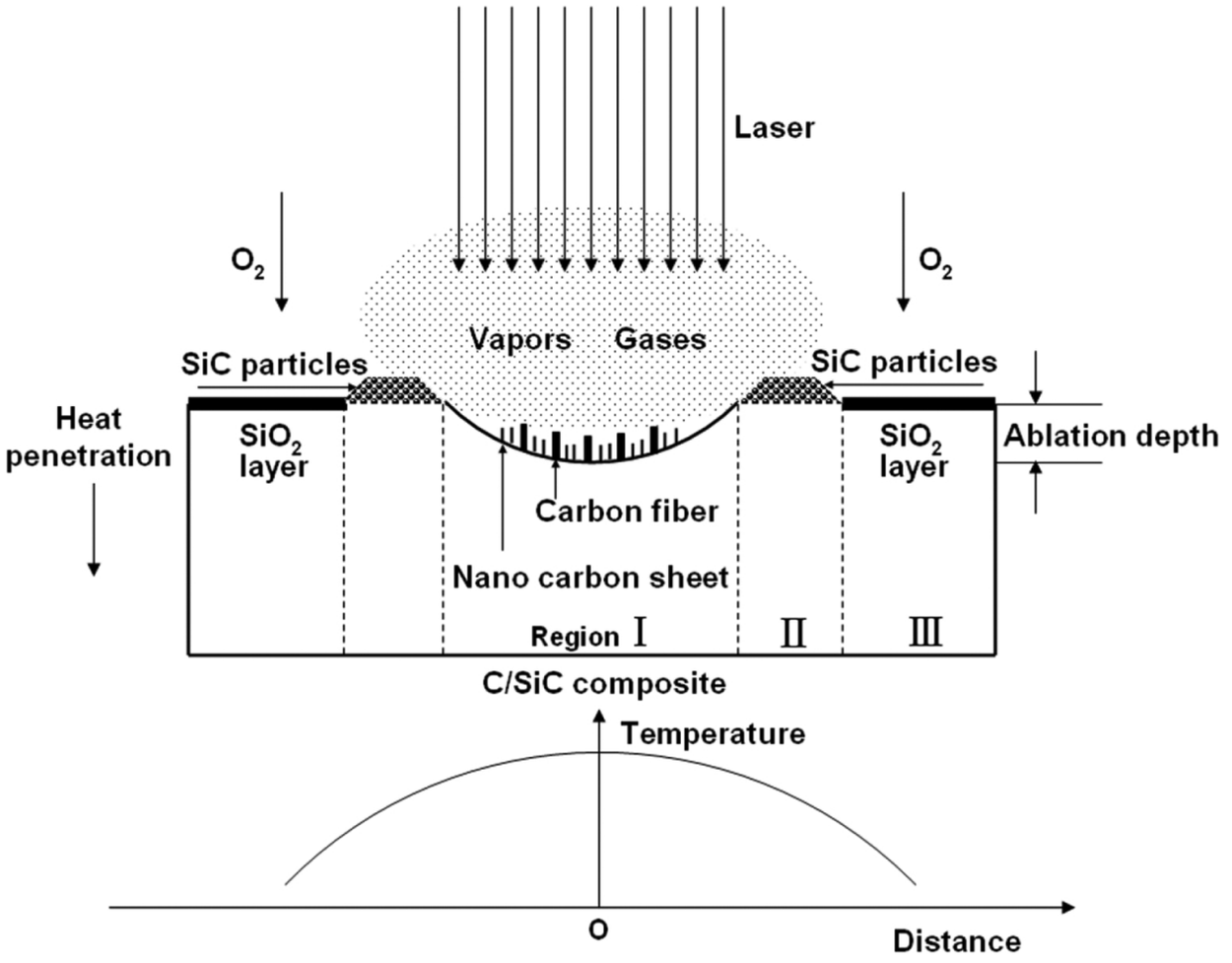

Figure 8. Schematic of the laser ablation processes.

http://dx.doi.org/10.5772/65108

carbon fibers where the temperature is high to decompose the SiC matrix but is not high enough to sublimate carbon fibers. The laser ablation of C/SiC composite in this center area is dominated by the decomposition and simulation process.

With the proceeding of the laser ablation, the positive gases escape from the surface of the ablated center due to the positive atmosphere produced by the decomposition, sublimation, and oxidation in the center region. Some gases deposit at the transitional zone (region II) where the temperature is relatively low and not high enough to lead to the decomposition of SiC phase. SiC grains re-nucleate and grow to spherical particles at the transitional zone, and the region becomes protuberant on the ablated surface.

At the ablation edge (region III), the heat is only conducted form the ablation center, and the temperature is the lowest among the three ablated regions. The temperature in this region cannot lead to the decomposition and sublimation of the phases. The C/SiC composite in this area is only oxidized and is covered by a white glassy SiO_2 layer. The oxidation products of C/SiC composite include CO, CO_2, SiO, and SiO_2. CO, CO_2, and SiO are gaseous and escape from the ablated surface. SiO_2 formed during the oxidation is in the liquid state at such a temperature, which can flow on to the carbon fibers and protects the C/SiC composite from further oxidation damage. The laser ablation of C/SiC composite in this region is dominated by the oxidation reaction of the composite with the atmosphere.

4.1.5. Laser ablation testing of C/C-ZrC composite

Due to the higher melting temperature and high-temperature ablation resistance of ZrC compared with SiC, we produced a C/C-ZrC composite and tested the ablation resistance of the as-produced C/C-ZrC composite using an impulse laser beam. The ablation resistance of C/SiC composite was also tested in the same parameters for comparison.

Figure 9 shows the linear ablation rates of C/C-ZrC composite and C/SiC composite versus the laser power densities. Both the linear ablation rates of the composites increase with increasing laser power densities. The linear ablation rates of C/C-ZrC composite are smaller than that of C/SiC composite. With increasing laser power densities, the difference of linear ablation rates between the two composites increases, which indicates that the ablation resistance of the C/C-ZrC composite is greatly improved at higher temperatures.

The much better ablation resistance of C/C-ZrC composite can be also illustrated by observing the morphologies of the ablated surface. As shown in **Figure 9**, the ablated surface of C/C-ZrC composite is covered by a white melting ZrO_2 layer (determined by EDS) without obvious ablation pit, while the C/SiC composite is severely ablated with a deep ablation pit without any protecting layer on the ablated surface. ZrO_2 owns a high melting point (2700 °C), low oxygen penetration rate, and excellent ablation resistance, which can act as a protecting layer for the C/C-ZrC composite, and thus, C/C-ZrC composite presents much better ablation resistance than the PIP C/SiC composite.

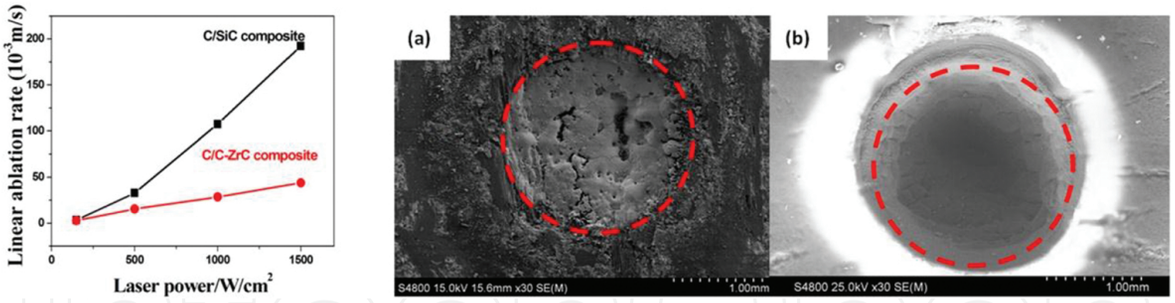

Figure 9. Linear ablation rates and macro-morphologies of (a) C/C-ZrC composite and (b) C/SiC composite after laser testing.

Materials	Test length (s)	Heat flux (W/cm²)	Blackbody temp (°F)	Adjusted temp (°F)	Weight change/area (g/in²)
C/ZrC	300	600	4858	5200	−0.029
C/Zr-Si-C	125	500	4556	4875	−0.051

Table 2. Laser-testing parameters and weight changes of the composites before and after testing.

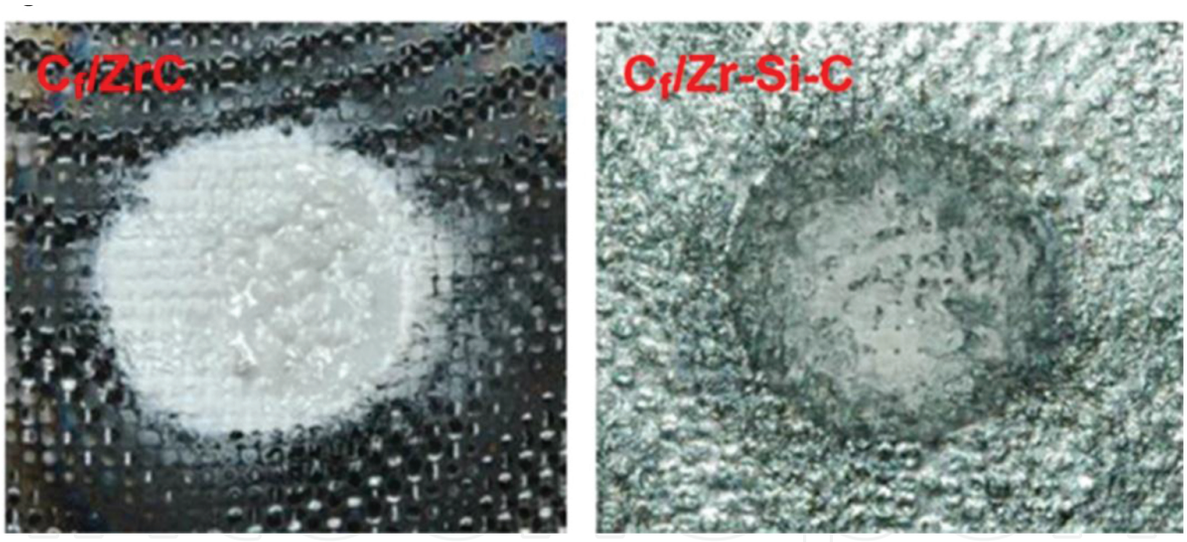

Figure 10. Surface morphologies of C/ZrC and C/Zr-Si-C composites after laser ablation testing.

Because of the excellent properties of carbon fiber-reinforced ZrC-based composites and their potential applications in hypersonic aerospace vehicles, Ultramet [26] developed a fast and economic reactive melt infiltration method to prepared C/ZrC and C/Zr-Si-C composites. Ablation resistance of the composites was tested using a continuous laser beam. Both C/ZrC and C/Zr-Si-C composites survived laser testing at 2871 °C and 2691 °C, respectively, under forced air flow at the Air Force Laser Hardened Materials Evaluation Laboratory. The testing parameters and weight changes of the composites before and after testing are shown

in **Table 2**. The composites show small weight change and excellent oxidation stability. Continuous protecting layers were formed on the ablated surface of C/ZrC and C/Zr-Si-C composites (**Figure 10**) and effectively protected the composites from severely ablation damage. Wang et al. [27] also prepared C/C-ZrC composite by reactive melt infiltration of liquid zirconium. They used a continuous wave CO_2 laser (ROFIN DC080W, Germany) to test the ablation resistance of the composite. The ablation depth increased with the increase in laser power densities. The reactive melt-infiltrated C/C-ZrC composite presented much better ablation resistance than C/C composite.

4.2. Ultra-high-temperature ceramics and coatings

Owing to their high melting temperatures, good chemical stability and excellent oxidation, and ablation resistance at elevated temperatures, ultra-high-temperature ceramics have captured great attentions and have potential application in extreme aerothermal and nuclear power-generation environments. Laser heating, known as rapid heating and high power density, is a convenient technique to test the ablation resistance of ultra-high-temperature ceramics.

Yan et al. [28] prepared an ultra-high-temperature ceramic-based composite ZrB_2/20SiC-Cu by spark plasma-sintering method and investigated the ablation behavior of the composite using a 20 MW/m^2 high-intensity continuous laser beam. They characterized the phase and microstructure evolution of the composite during ablation with XRD and SEM. The results revealed that no macroscopic damage but only an ablated layer was observed after being ablated. The composite exhibited good ablation resistance against high-intensity continuous laser beam. Cu phase in the composite evaporated preferentially, and a ZrO_2 layer with different forms such as closely packed nanoparticle and melting layer was generated at the laser spot center. Dendrites and columnar ZrO_2 grains were found on the cross section morphologies of the composite after ablation, which further demonstrated the melting of ZrO_2 layer during ablation. The liquid ZrO_2 layer had capability of thermal insulation, which prevented the inner matrix from further ablation. Both the state transformation of Cu and generated ZrO_2 dissipated a lot of energy, which was another important reason why ZrB_2/20SiC-Cu composite had good ablation resistance in such ablation condition.

Due to the rapid achieving of ultra-high temperatures, Jayaseelan et al. [29] used a laser beam to heat and melt ultra-high-temperature ceramics. The laser beam is a 3 kW Nd:YAG laser with a 10 mm diameter collimated beam capable of delivering a heat flux of up to~20 MW/m^2. Sample temperature was recorded by a pyrometer (Raytek 1MH) with a measurement range of 650 and 3000 °C. They investigated the microstructural evolution of spark plasma-sintered ZrB_2, ZrB_2/20 vol.% SiC (ZS20), and ZrC ultra-high-temperature ceramics (UHTCs) during laser heating. Laser heating at temperatures between 2000 and 3750 °C resulted in extensive bubble and crater formation on the surfaces of 10 mm diameter samples (**Figure 11**). Only crystalline zirconia with a wide range of morphologies including nodules, needles, nanofibers, and lamella was formed on the surface of ZrB_2 and ZS20 samples laser heated in air up to 2700 °C (**Figure 11**). The surface of ZrC samples after laser heated in vacuum up to 3750 °C was characterized by dendritic and eutectic morphologies. Solidification cracks and

trapped porosity were also observed on the samples' surface. A complex array of mechanisms involving solid, liquid, and vapor phases led to formation of these morphologies including melting, oxidation, volatilization, and liquid flow.

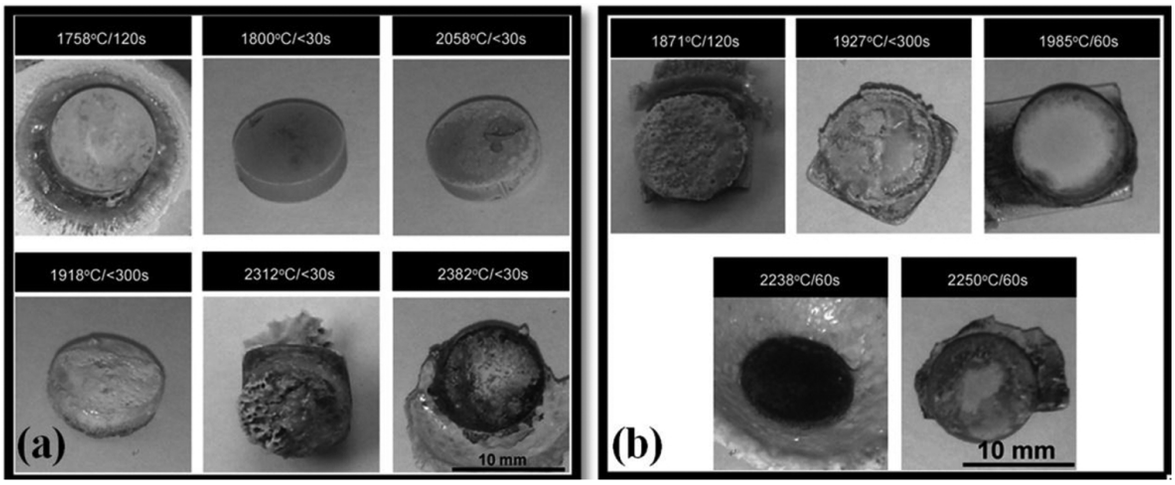

Figure 11. Macro-morphologies of laser-heated (a) ZrB_2/20 vol.% SiC and (b) ZrB_2 samples.

In addition to the laser ablation of ultra-high-temperature ceramics, the laser beams were also used to characterize the ablation resistance of ultra-high-temperature ceramic coatings. Liu et al. [30] prepared a two-layer SiC-ZrC coating on C/C composite by chemical vapor deposition method. They characterized the ablation resistance of the coating using a continuous CO_2 laser beam and investigated the laser ablation behaviors and ablation mechanisms of the SiC-ZrC-coated C/C composites. The results indicated that the ablation depth and width increased with increasing the laser power. Laser ablation resistance of the composites was greatly improved by the SiC-ZrC coating. They found three ablation regions on the ablated coating surface and discussed the formation mechanism. At the ablation center, the ablation was thought to be dominated by the blast and sublimation processes. At the transitional zone, the main ablation mechanism was evaporation. At the ablation edge, the ablation was mainly controlled by the oxidation process. Li et al. [31] also employed the laser beam to characterize ablation resistance of ultra-high-temperature ceramic coatings. A TaC coating was prepared on C/C composite by chemical vapor deposition to improve ablation resistance of the composite at high temperatures. They tested the ablation resistance of TaC coating and investigated ablation mechanism.

5. Conclusions

Laser ablation is a facile, reliable, and economical method to evaluate ablation resistance of materials. The fundamentals of laser-material interactions were discussed from the physical aspects and chemical aspects. The physical aspects mainly involved the absorption of laser radiation, heating and propagation, melting, vaporization, and solidification. The chemical aspects mainly involved the decomposition of materials and the reaction between the materials

and the testing atmosphere. Some practical applications of laser ablation in ablation-resistance characterization of ultra-high-temperature ceramics and composites were presented, and the ablation behavior and mechanism were discussed.

Author details

Yonggang Tong[1,2*], Xiubing Liang[1], Shuxin Bai[2] and Qing H. Qin[3]

*Address all correspondence to: tygiaarh419@163.com

1 National Engineering Research Center for Mechanical Product Remanufacturing, Academy of Armored Forces Engineering, Beijing, China

2 College of Aerospace Science and Engineering, National University of Defense Technology, Changsha, China

3 Research School of Engineering, Australian National University, Canberra, Australia

References

[1] Malek C. Laser processing for bio-microfluidics applications. Anal. Bioanal. Chem. 2006;385:1351–1361.

[2] Kontinos DA, Gee K, Prabhu DK. Temperature constraints at the sharp leading edge of a crew transfer vehicle, AIAA 2001-2886.

[3] Zhao D, Zhang CR, Hu HF, Zhang YD. Ablation behavior and mechanism of 3D C/ZrC composite in oxyacetylene torch environment. Compos. Sci. Technol. 2008;71(11):1392–1396.

[4] Zhang X, Hu P, Han J, Meng S. Ablation behavior of ZrB_2–SiC ultra high temperature ceramics under simulated atmospheric re-entry conditions. Compos. Sci. Technol. 2008;68:1718–1726.

[5] Monteverde F, Savino R, Fumo MDS, Maso AD. Plasma wind tunnel testing of ultra-high temperature ZrB_2–SiC composites under hypersonic reentry conditions. J. Eur. Ceram. Soc. 2010;30:2313–2321.

[6] Tang SF, Deng JY, Wang SJ, Liu WC, Yang K. Ablation behaviors of ultra-high temperature ceramic composites. Mater. Sci. Eng. A 2007;465:1–7.

[7] Shen XT, Li KZ, Li HJ, Fu QG, et al. The effect of zirconium carbide on ablation of carbon/carbon composites under an oxyacetylene flame. Corros. Sci. 2011;53:105–112.

[8] Dahotre NB, Harimkar SP. Laser Fabrication and Machining of Materials. New York: Springer, 2008.

[9] Ready JF. Industrial Applications of Lasers. San Diego: Academic Press, 1997.

[10] Steen W, Mazumde J. Laser Materials Processing. London: Springer, 2010.

[11] Lide DR. CRC Handbook of Chemistry and Physics. Boca Raton: CRC, 2001.

[12] Wu CW, Wu XQ, Huang CG. Ablation behaviors of carbon reinforced polymer composites by laser of different operation modes. Opt. Laser Technol. 2015;73:23–28.

[13] Schaaf P. Laser Processing of Materials: Fundamentals, Applications and Developments. Berlin: Springer, 2010.

[14] Bulgakova NM, Bulgakov AV. Pulsed laser ablation of solids: transition from normal vaporization to phase explosion. Appl. Phys. A 2001;73:199–208.

[15] Zhou RF, Han YF, Li SS. High Temperature Structure Materials. Beijing: National Defend Industry Press, 2006.

[16] Wilson J, Hawkes JF. Lasers: Principles and Applications. New York: Prentice-Hall, 1987.

[17] Oliveira V, Colaco R, Vilar R. Simulation of KrF laser ablation of Al_2O_3–TiC. Appl. Surf. Sci. 2007;253:7585–7590.

[18] Bäuerle D. Laser Processing and Chemistry. Berlin: Springer, 2000.

[19] Clauer AH, Fairand BP, Wilcox BA. Laser shock hardening of weld zones in aluminum alloys. Metall. Trans. A 1977;8(12):1871–1876.

[20] Ultramet. Ceramic Matrix Composites [Internet]. Available from: http://www.ultramet.com/ceramic_matrix_composites.html

[21] Pan YS, Xu YD, Chen ZF, Chen LF, Zhang LT, Xiong DS. Ablation properties analysis of 2D C/SiC composites. Ordnance Mater. Sci. Eng. 2006;29:17–21.

[22] Jian K, Chen ZH, Ma QS, Hu HF, Zheng WW. Effects of polycarbosilane infiltration processes on the microstructure and mechanical properties of 3D-Cf/SiC composites. Ceram. Int. 2007;33:905–909.

[23] Tong YG, Bai SX, Zhang H, Ye YC. Laser ablation behavior and mechanism of C/SiC composite. Ceram. Int. 2013;39:6813–6820.

[24] Fang D, Chen ZF, Song YD, Sun ZG. Morphology and microstructure of 2.5 dimension C/SiC composites ablated by oxyacetylene torch. Ceram. Int. 2009;35:1249–1253.

[25] Yudasaka M, Komatsu T, Ichihashi T, Iijima S. Single wall carbon nanotube formation by laser ablation using double-targets of carbon and metal. Chem. Phys. Lett. 1997;278:102–106.

[26] Ultramet. Ceramic Matrix Composites [Internet]. Available from: http://www.ultramet.com/ceramic_matrix_composites_performance.html

[27] Wang YG, Zhu XJ, Zhang LT, Cheng LF. Reaction kinetics and ablation properties of C/C–ZrC composites fabricated by reactive melt infiltration. Ceram. Int. 2011;37(4):1277–1283.

[28] Yan ZY, Ma Z, Liu L, Zhu SZ, Gao LH. The ablation behavior of ZrB_2/Cu composite irradiated by high-intensity continuous laser. J. Eur. Ceram. Soc. 2014;34:2203–2209.

[29] Jayaseelan DD, Jackson H, Eakins E, Brown P, Lee WE. Laser modified microstructures in ZrB2, ZrB2/SiC and ZrC. J. Eur. Ceram. Soc. 2010;30:2279–2288.

[30] Liu QM, Zhang LT, Jiang FR, Liu J, Cheng LF, Li H et al. Laser ablation behaviors of SiC-ZrC coated carbon/carbon composites. Surf. Coat. Technol. 2011;205(17–18):4299–4303.

[31] Li GD, Xiong X, Huang KL. Ablation mechanism of TaC coating fabricated by chemical vapor deposition on carbon-carbon composites. Trans. Nonferrous Met. Soc. China 2009;19:689–695.

IntechOpen